Electric Power Systems Research 216 (2023) 108968

Contents lists available at ScienceDirect

Electric Power Systems Research

journal homepage: www.elsevier.com/locate/epsr

The Johannesburg Lightning Research Laboratory, Part 3: Evaluation of the South African Lightning Detection Network

Haydn Fensham [a], Hugh G.P. Hunt [a,*], Carina Schumann [a], Tom A. Warner [b], Morne Gijben [c]

[a] Johannesburg Lightning Research Laboratory, School of Electrical and Information Engineering, University of Witwatersrand, Johannesburg, South Africa
[b] ZTResearch, Rapid City, SD, USA
[c] South African Weather Service, Pretoria, South Africa

ARTICLE INFO

Keywords:
Lightning
SALDN
Performance evaluation
Detection efficiency
Location accuracy
High-speed videography

ABSTRACT

This research describes an approach to evaluating the performance of the South African Lightning Detection Network (SALDN) over Johannesburg, South Africa, using high-speed video footage of lightning events. The performance evaluation includes the flash detection efficiency, stroke detection efficiency and median location accuracy (locations of known attachments and flash cluster approach) of the SALDN. The proposed methodology has three subsections: time-correlating cloud-to-ground stroke data from the SALDN with ground truth lightning events (high-speed camera footage), determining the detection efficiency and determining the location accuracy. Results indicate that the SALDN has a flash detection efficiency of 84.9%, stroke detection of 69.1% and has a median location accuracy of 59.2 m and 124.4 m using locations of known attachments and flash cluster approaches respectively for cloud-to-ground lightning over Johannesburg.

1. Introduction

The South African Lightning Detection Network (SALDN) operated by the South African Weather Service (SAWS) was first put into operation in 2006. There was a performance evaluation on the SALDN in 2014 [1]. However, the stroke detection efficiency was not obtainable and the location accuracy was found for only one location. This means the stroke detection efficiency of the SALDN is unknown and the location accuracy is unknown over a greater region. In this paper, we compare stroke reports from the SALDN with high-speed video observations of lightning over Johannesburg, South Africa as found in [2–5].

2. Performance of an LLS

The main performance measure of an LLS is the detection efficiency and location accuracy [6]. As discussed before, a flash consists of multiple strokes. The DE can be defined in terms of two parameters, the flash DE and the stroke DE. The flash DE is the percentage of flashes detected by the network versus the number of ground truth flashes. The stroke DE is the percentage of strokes (1st RS and SRSs) detected by the network versus the number of ground truth strokes. The flash and stroke DE gives an indication of how well the LLS is detecting lightning. The flash DE will be greater than that of the stroke DE because the LLS only needs to detect one of the strokes in a given flash in order to detect this flash [7]. LLSs provide a reported location of a detected lightning event. Location error is the distance between the actual location of a lightning event and the reported LLS location of the lightning event. An illustration of this can be seen in Fig. 1. The LA is a dataset of multiple location errors which can represented by using statistics such as the maximum, minimum, median, standard deviation, mode and mean of the location errors [1].

The European LLS, EUCLID (European Cooperation for Lightning Detection) was evaluated using various ground truth data. The LA, DE and current estimations of EUCLID were evaluated. The LA was calculated by using the Gaisberg Tower measurement system and the data obtained from EUCLID. With the lightning terminating on the tower, the actual location of the lightning event was known and this could be compared to the location estimated from EUCLID. The DE was presented using two different methods, the first being the instrumented tower and the second being the video and E-field data. The flash DE and stroke DE was found to be 96% and 70% using the Gaisberg Tower. In Austria, EUCLID had a flash DE and stroke DE of 98% and 84% using high-speed cameras for flashes to the tower which had at least one SRS. With improvements to the LLS, the last 100 strokes on the Gaisberg Tower had a median LA of 89 m. There has been a continuous improvement to the LA of EUCLID with software and hardware improvements [8]. In Hong Kong, the LLS in operation is the Guangdong–Hongkong–Macau Lightning Location System (GHMLLS).

* Corresponding author.
E-mail address: hugh.hunt@wits.ac.za (H.G.P. Hunt).

https://doi.org/10.1016/j.epsr.2022.108968
Received 5 September 2022; Received in revised form 24 October 2022; Accepted 11 November 2022
Available online 6 December 2022

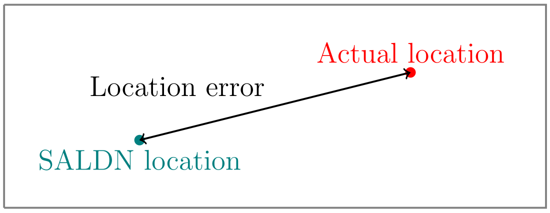

Fig. 1. Location error (m) between SALDN location and actual location.

The flash DE, stroke DE, LA and peak current estimation accuracy of the GHMLLS was evaluated. Two methods were used to gather ground truth data. The first was lightning triggered experiments which took place in Conghua and the second was the observation of natural flashes on tall structures using high speed video footage along with other sensors, which took place in Guangzhou. Data over many years was obtained and evaluated to determine the performance measures of the GHMLLS. The results obtained were: flash DE of 95%, stroke DE of 90% and median LA of 410 m. These results showed a significant improvement in the performance of the LLS after an upgrade in 2012 [6].

In Brazil, the LLS is referred to as the Brazilian Integrated Lightning Detection Network (RINDAT). This network has seen multiple upgrades to increase the DE and LA. A performance evaluation of the network used high-speed camera footage of negative downward flashes as the ground truth data. The RINDAT was found to have a flash DE of 87.4% and a stroke DE of 54.7%. These values were in agreement with the expected DE by the manufacturer. The LA was determined by taking the maximum distance between strokes within a flash. Thus, this LA is a overestimation of the network. The median LA was found to be 3.4 km. This was the first performance evaluation of the RINDAT where all sensors were operating normally [9]. The U.S. National Lightning Detection Network (NLDN) has had multiple performance evaluations where the DE, LA and peak current estimation accuracy were determined. These performance evaluations used rocket triggered lightning in the Florida region. The location errors were defined as the distance between the rocket launcher and the reported location of the lightning event from the NLDN. Using data from 2004 to 2013 the following results were obtained: The flash DE, stroke DE and median LA was 94%, 75% and 309 m respectively. These results show the constant improvement of the NLDN since performance evaluations in 2005, 2011 and 2014 [10]. In 2014, there was a performance evaluation on the SALDN using low-speed cameras, the flash DE was found to be 76% in the last season (2012–2013) with a median LA of 280 m for data collected between 2009-2013 [1].

3. Instrumentation and data

The ground truth performance evaluation of an Lightning Location System (LLS) requires two forms of data, ground truth lightning data and the LLS data. Ground truth lightning data is important as it provides evidence that a flash or stroke occurred. LLS data can be compared to ground truth lightning data to establish if the ground truth lightning event was detected or not. In this research, the ground truth lightning data is collected using high-speed video cameras over Johannesburg, South Africa. The LLS data is provided by the South African Weather Service and is in the form of Cloud-to-Ground (CG) stroke South African Lightning Detection Network (SALDN) data.

3.1. High-speed video investigation in Johannesburg

High-speed cameras are one way to gather ground truth lightning events [8]. They can capture videos at thousands of frames per second. This allows processes such as the leader and the strokes within a flash to be observed and analysed. The ground truth data for this research was collected using two high-speed cameras, the Phantom v310 (15 000 fps) and the Phantom v7.1 (5 000 fps), which overlook Johannesburg, South Africa (shown in Fig. 2). The high-speed cameras are positioned approximately 6 km away from Johannesburg city centre. Within the Johannesburg CBD there are two tall towers, the Telkom and Sentech Tower. The Telkom and Sentech Tower have a height of 270 m and 232 m respectively.

The high-speed camera investigation over Johannesburg collected data between the 5th February 2017 and 6th February 2018 during the summer season. Thunderstorms are expected during the summer season in Johannesburg, South Africa. The current in a channel (therefore the luminosity from that channel) can be used to distinguish different processes in a flash. The high-speed camera images in this subsection will help visualise these processes. Fig. 3 shows an example of a downward flash. The downward stepped leader is the first visible process as seen in the first image. It is important to note the branches on the stepped leader. The branches are pointing towards the earth like an upside down tree, indicating a downward flash. The second image shows attachment, which is associated with a large increase in luminosity over a short period of time (impulsive event). This can now be referred to as the 1st Return Stroke (RS) as seen in the third image. Once the luminosity of the 1st RSs channel ceases, there can be a dart leader looking for attachment down the ionised channel as seen in the fourth image. Once attachment is made, a Subsequent Return Stroke (SRS) is formed as seen in the fifth image. These videos also allow the duration of the continuing currents to be inferred.

Fig. 4 shows an example of an upward flash. The first visible stage is the upward leader. In the first image the upward leader has multiple branches as seen with the downward flash, however, these branches are facing the clouds. The second image shows a fluctuation in the luminosity of one of the branches. This is an Initial Continuous Current (ICC) pulse as discussed previously and is superimposed on the upward leader. Any luminosity fluctuation on an entire upward leader branch was considered an ICC pulse. Once the flow of current in the upward leader ceases, a dart leader can propagate down the channel. The third image illustrates the dart leader propagating towards earth. Once attachment is made, as seen in the fourth image, a large increase in luminosity is seen and the SRS is formed as seen in the fifth image. A positive upward flash is when a negative upward leader propagates towards the cloud base. Similarly, a negative upward flash is when a positive upward leader (i.e. when recoil leaders are visible) propagates towards the cloud base. Recoil leader are one of the characteristics that allow the polarity of a downward or upward flash to be determined from a high-speed video. If recoil leaders appear in the video, then the polarity of the channel is positive. If there are no recoil leaders, then the current of the channel is negative.

Table 1 shows an example of the ground truth data obtained from analysing a high-speed video. Row 1 and 4 of the data sheet are 1st return strokes because of the different strike points in the flash. This is a case of multiple ground contacts within a flash. The remaining strokes are subsequent return strokes. In the case where there was a CG triggered upward flash, the triggering event was considered as a downward flash. This means the triggering event was not classified as part of the upward flash.

Table 2 summarises the ground truth data captured over Johannesburg. 206 flashes and 667 strokes were recorded during the 24 thunderstorms. Of the 206 flashes, 163 are downward flashes and 43 are upward flashes. The majority of these upward flashes occurred on the Telkom and Sentech Tower. The data show that there were 55 upward leaders which is greater than the amount of upward flashes. This means that certain upward flashes had multiple upward leaders coming from different objects on the ground. An interesting observation is the large amount of ICC pulses which were recorded. On average there are 9 ICC pulses per upward flash.

Fig. 2. Image showing the setup of the high-speed cameras.

Fig. 3. The different processes in downward flashes caught with a high-speed camera.

Fig. 4. The different processes in upward flashes caught with a high-speed camera.

Table 1
High-speed video of a downward flash analysed into a data sheet.

Time	Process	Strike point	Polarity	Visible	Duration (ms)
14:58:34:070	Stroke	1	Negative	yes	7
14:58:34:103	Stroke	1	Negative	yes	6
14:58:34:121	Stroke	1	Negative	yes	5
14:58:34:208	Stroke	2	Negative	no	
14:58:34:256	Stroke	2	Negative	no	
14:58:34:292	Stroke	2	Negative	no	

Table 2
High-speed camera data (ground truth data).

Lightning events	High-speed camera events
Thunderstorms	24
Flashes	206
Strokes	667
Downward flashes	163
Strokes	604
M-components	101
Upward flashes	43
Upward leaders	55
ICC pulses	387
Subsequent Return Strokes	63
M-components	10

3.2. The South African Lightning Detection Network

The SALDN is owned by the South African Weather Service. The SALDN was established in 2005 and consisted of 19 sensors. In 2010, 3 sensors were added to the network. In 2011, 2 sensors where added and 2 sensors were relocated. Currently the SALDN consists of 25 Vaisala LS7000 sensors which are positioned as seen in Fig. 5 [1]. The sensors have a mean distance of approximately 250 km between the each other. The self-evaluated performance of the SALDN is 90% for the flash DE and 0.5 km for the median location accuracy [11]. Changes to the network over the study period have been as follows:

- Addition of the Wolwespruit sensor in 2015
- Moved the sensor at Durban Virginia airport to Vernon Crookes Golf Course
- Upgraded the Total Lightning Processor (TLP) in August 2019

Fig. 5. Location of the 25 Vaisala sensors in South Africa as of 2022 [1]. The location of Johannesburg, where the Sentech and Telkom towers are located, is indicated by the red circle.

Table 3
SALDN data which detected a downward flash.

Time	lat	lon	peak_kA	chi_square	num_dfrs
14:58:34:071	−26.1770	27.9882	−21	0.6	12
14:58:34:104	−26.1778	27.9873	−24	1.4	3
14:58:34:121	−26.1770	27.9883	−9	0.3	6
14:58:34:208	−26.1762	27.9773	−23	0.5	13
14:58:34:256	−26.1760	27.9772	−16	0.2	8
14:58:34:292	−26.1762	27.9770	−13	0.4	7

The self-evaluated performance is based on a model assuming certain values for each sensor detection efficiency as a function of peak current and distance and the median error ellipse calculations of downward flashes.

In 2014, the performance of the SALDN was evaluated using low-speed camera footage of CG flashes terminating on the Sentech Tower [1]. The flash DE and the LA of the SALDN was determined. However, with the use of a low-speed camera, the stroke DE could not be determined as individual strokes could not be observed. Secondly, the only flashes which were captured were those that terminated on the Sentech Tower. Therefore the flash DE and LA were calculated for only one location. Lastly, only lightning events terminating on the Sentech Tower were gathered meaning the results are based on predominately upward flashes.

SALDN CG stroke data were obtained for the 24 thunderstorms in the ground truth data. The data for the region −26.0° to −26.5° Latitude and 27.8° to 28.3° Longitude. This area was chosen as it enclosed the field of view of the cameras and also allowed for errors which might occur in the SALDN reported locations. 26 598 strokes were detected by the SALDN in the filtered area for the 24 thunderstorms which the cameras collected data from. Table 3 gives an example of the filtered SALDN data. In this case the data were already time-correlated to the video data in Table 1. The table shows the data which is provided by the SALDN. Each stroke contains the time (Time) at which the event occurred, the latitude (lat) and longitude (lon) of the lightning event, the peak current (peak_kA), chi square (chi_square) value and number of detected sensors (num_dfrs).

4. Performance Evaluation Methodology

This methodology is a general method to finding the Detection Efficiency (DE) and Location Accuracy (LA) of an Lightning Location System (LLS) using ground truth lightning events. The detection efficiency includes the flash and stroke detection efficiency. The location accuracy includes determining the location accuracy using lightning events which attached to known locations as well as by using a flash cluster method. The methodology requires GPS time stamped Cloud-to-Ground (CG) LLS stroke data and GPS time stamped ground truth lightning event data. Ground truth lightning data can be collected from not only high-speed videos but by instrumented towers or rocket triggered lightning [8]. However, for the flash cluster method used to find the location accuracy, the ground truth data will need to provide evidence that the strokes are within the same channel and therefore have the same Ground Strike Point (GSP). It can be seen from high-speed videos if strokes have the same channel and therefore the same ground strike point.

4.1. Time-correlation of LLS data and ground truth lightning events

The following methodology is used to time-correlate CG LLS stroke data and ground truth lightning events. This time-correlation between LLS data and ground truth lightning events forms a *time-correlated dataset* in which the lightning events within the video have either been noted as detected or not detected by the SALDN.

1. Create a dataset of the recorded ground truth lightning events, referred to as the *ground truth dataset*:

- GPS time stamp of the lightning event.
- Type of lightning (leaders, strokes, M-components, ICC pulses, positive or negative current polarity).
- Number of strike points.
- Duration of the strokes.
- Note if lightning event attached to a structure of interest.

2. Filter the CG LLS stroke data by date, time and area of the thunderstorms in which ground truth lightning events were captured. This data will be referred to as the *filtered LLS dataset*.
3. Time-correlate the *ground truth dataset* and the *filtered LLS dataset*. If the filtered LLS data detected the same lightning event as the ground truth data, indicate this and insert the coordinates of the flash given by the LLS data next to that entry in the *ground truth dataset*. This completed dataset will now be referred to as the *time-correlated dataset*.

4.2. Determining the detection efficiency

The *time-correlated dataset* is used to determine the flash DE and the stroke DE of an LLS. The following methodology is used to determine the flash DE from the *time-correlated dataset*.

1. Determine the number of ground truth flashes in the *time-correlated dataset*.
2. Determine if any lightning events in a flash were detected by the LLS. If so, indicate that the flash has been detected in the *time-correlated dataset*.
3. Calculate how many flashes were detected by the LLS in the dataset. This is the number of detected LLS flashes in the *time-correlated dataset*.
4. Using Eq. (1) calculate the flash detection efficiency.

$$\mathrm{D}E_{Flash} = \frac{no.\ detected\ LLS\ flashes\ in\ time\ correlated\ dataset}{no.\ ground\ truth\ flashes\ in\ time\ correlated\ dataset}\% \tag{1}$$

The following methodology is used to determine the stroke DE from the *time-correlated dataset*. Stroke refers to 1st Return Stroke (RS) and Subsequent Return Stroke (SRS) for downward flashes as well as SRS for upward flashes.

1. Determine the number of ground truth strokes in the *time-correlated dataset* for downward and upward flashes.
2. Calculate the total number of strokes which were detected by the LLS data in the *time-correlated dataset*. This is the number of detected LLS strokes in the *time-correlated dataset*.
3. Using Eq. (2) calculate the stroke detection efficiency.

$$\mathrm{D}E_{Stroke} = \frac{no.\ detected\ LLS\ strokes\ in\ time\ correlated\ dataset}{no.\ ground\ truth\ strokes\ in\ time\ correlated\ dataset}\% \tag{2}$$

4.3. Determining the location accuracy

Two approaches are used in this methodology to evaluate the location accuracy. The first method utilises known locations where strokes have terminated and the second is using the differences in reported locations of SRSs with regards to the 1st RS that occurred in the same channel within a flash (flash cluster).

4.3.1. Locations of known attachment

The LA can be found by using lightning events which have terminated on known locations. Since the location of the structure is known, the location error between the structure and the reported LLS location can be determined. This method requires entries in the *time-correlated dataset* that have terminated on known locations and have been detected by the LLS.

1. From the *time-correlated dataset*, create a subset of data which only includes detected lightning events which terminated on the known locations. This will be referred to as the *known location dataset*.
2. Calculate the location errors in metres between the coordinates of the known location and the coordinates given by the LLS data for the lightning events.
3. Determine the maximum, minimum, median, standard deviation, mode and arithmetic mean of the calculated location errors.

4.3.2. Flash cluster

The flash cluster method is described by Schulz et al. [12]. The method determines the LA by using Negative Cloud-to-Ground (nCG) flashes. The high-speed cameras allow one to determine if the 1st RS and SRSs are in the same channel and therefore can be assumed to have the same GSP, meaning they terminate at the same location. Ideally, the LLS should report all the locations of the 1st RS and SRS as the same since they terminate at the same GSP. However, there are differences between these reported locations and the location error can be found between the different locations [12].

The stroke with the highest peak current estimate within a flash can be considered to the most accurately located stroke since it is more likely to be detected by multiple sensors. The more sensors that detect a stroke the better the LA of that stroke [13]. The 1st RS generally has the highest peak current in a flash and therefore can be considered the most accurate location of the flash. The difference in reported locations between the 1st RS and the SRSs in the flash form the dataset of location errors. The statistics of the LA can then be calculated.

Fig. 6a, gives an example of how the location error is defined. Fig. 6b, is the same flash represented in Fig. 3. The flash consisted of 5 strokes. The red number 1 illustrates the 1st RS and the blue number 2 represents the first SRS as seen in Fig. 3. This is seen as the flash cluster. The high-speed camera was used to determine if all the SRS strokes were in the same channel.

Fig. 7, shows the flow diagram used to determine the LA using the flash cluster approach. The method requires the *time-correlated dataset* and requires flashes within that dataset to have the 1st RS detected as well as a minimum of one SRS detected. If this is satisfied, the geographical location of the flash should be that of the 1st RS. Then the location errors between the flash location and the SRSs need to be calculated for all the flashes. Once all the flashes that meet the criteria have been processed, the LA can be calculated from the location errors.

5. Results

These results are the performance evaluation of the South African Lightning Detection Network (SALDN) which include the flash Detection Efficiency (DE), stroke detection efficiency and Location Accuracy (LA). The results can be compared to the self-evaluation index of the SALDN as well as other performance evaluations of Lightning Location Systems (LLS). This will provide a reference as to how well the system performs. This data can also be used in future research to compare with a performance evaluation of an upgraded SALDN.

5.1. Time-correlated data

The *time-correlated data* can be seen in Table 4. This data allows the DE to be calculated. The high-speed camera events column refers to the ground truth data that was recorded and analysed. The SALDN events column refers to the SALDN stroke data that was time-correlated with the ground truth data. As seen in the table, 175 flashes were detected by the SALDN out of 206 filmed flashes, 457 strokes were detected by the SALDN out of 667 filmed strokes.

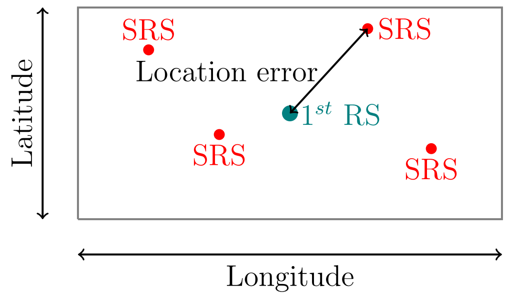

(a) The location error within a flash cluster

(b) Captured and detected flash cluster

Fig. 6. The location error within a flash cluster and an example of a flash cluster captured in this research.

Table 4
Time-correlated data of the high-speed video camera data and the SALDN data.

Lightning events	High-speed camera events	SALDN events	Percentage
Flashes	206	175	84.9%
Strokes	667	457	68.5%
Downward flashes	163	151	92.6%
Strokes	604	417	69.0%
M-components	101	12	–
Upward flashes	43	24	55.8%
Upward flash DE (SRS)	16	15	93.7%
Upward flash DE (no SRS)	27	9	33.3%
Upward stroke DE	63	40	63.4%

5.2. Detection efficiency

The SALDN detected 175 flashes of the 206 flashes that were filmed using the high-speed camera as seen in Table 4. This includes both downward and upward flashes and these are shown as a bar graph in Fig. 8. The first bar represents downward flashes and the second bar represents upward flashes. Flashes detected by the SALDN are shown in green and lashes captured by the high-speed cameras are shown in blue. The SALDN detected 151 downward flashes ofthe 163 filmed flashes (92.6%). Upward flashes can be categorised into upward flashes with Subsequent Return Strokes (SRSs) and upward flashes without SRSs. Upward flashes with SRSs were detected 93.7% of the time whereas upward flashes without SRS were detected 33.3% of the time.

5.3. Stroke detection efficiency

A total of 667 strokes were filmed by the high-speed cameras, of this, 457 strokes were detected by the SALDN. The SALDN has a stroke DE of 68.5%. This can also be seen in Fig. 9. The first bar represents downward strokes (1st return strokes and subsequent return strokes) and the second bar represents strokes in upward initiated flashes (subsequent return strokes). The red aspect of the bars represent the number of strokes detected by the SALDN and the grey represents the number of strokes captured on the high-speed cameras. Within the downward flashes, strokes (1st return strokes and subsequent return strokes) are of interest. It can be seen that the DE for a downward stroke is 69.0%. Upward strokes refer to the SRSs which can occur in an upward flash. The upward stroke DE is 63.4%.

6. Location accuracy

Two methods have been used to determine the LA of the SALDN. The first is the use of locations of known attachment and the second is the flash cluster method.

6.1. Locations of known attachment

This method required known locations where lightning had terminated. In this research the locations of known attachment were the Sentech and telkom Tower. These two locations provided the true coordinates of the attachment of the lightning event which could be compared to the locations reported by the SALDN. Fig. 10 shows the locations of the cameras and the Sentech and Telkom Tower with the y-axis indicating the latitude and the x-axis indicating the longitude. The reported locations of the lightning events which terminated on the towers have also been plotted. Note the reports with large location errors. These outliers are discussed in more detail in the discussion section.

Table 5 below gives the overall location accuracy for both towers and the location accuracy for each tower separately. As seen in the table, a total of 98 detected strokes and ICC pulses terminated on the towers. With these 98 events the SALDN has a median LA of 59.2 m.

6.1.1. Sentech tower

45 detected strokes and ICC pulses terminated on the Sentech Tower. Fig. 11 shows the reported locations of the events around the tower with the y-axis and x-axis as a distance in metres. The reported SALDN locations are grouped within 450 m of the tower. This figure excludes the one large location error seen in Fig. 10. Table 6 shows that the SALDN has a median location accuracy of 74.7 m at the Sentech Tower.

6.1.2. Telkom Tower

53 detected strokes and ICC pulses terminated on the Sentech Tower. Fig. 12 illustrates the distance in metres between the reported locations and the Telkom Tower. The x and y-axis are a distance in metres and the reported SALDN locations are grouped within 550 m of the tower. As with the Sentech Tower this figure excludes one large location error which is seen in Fig. 10. Table 7 shows that the SALDN has a median location accuracy of 51.0 m at the Telkom Tower.

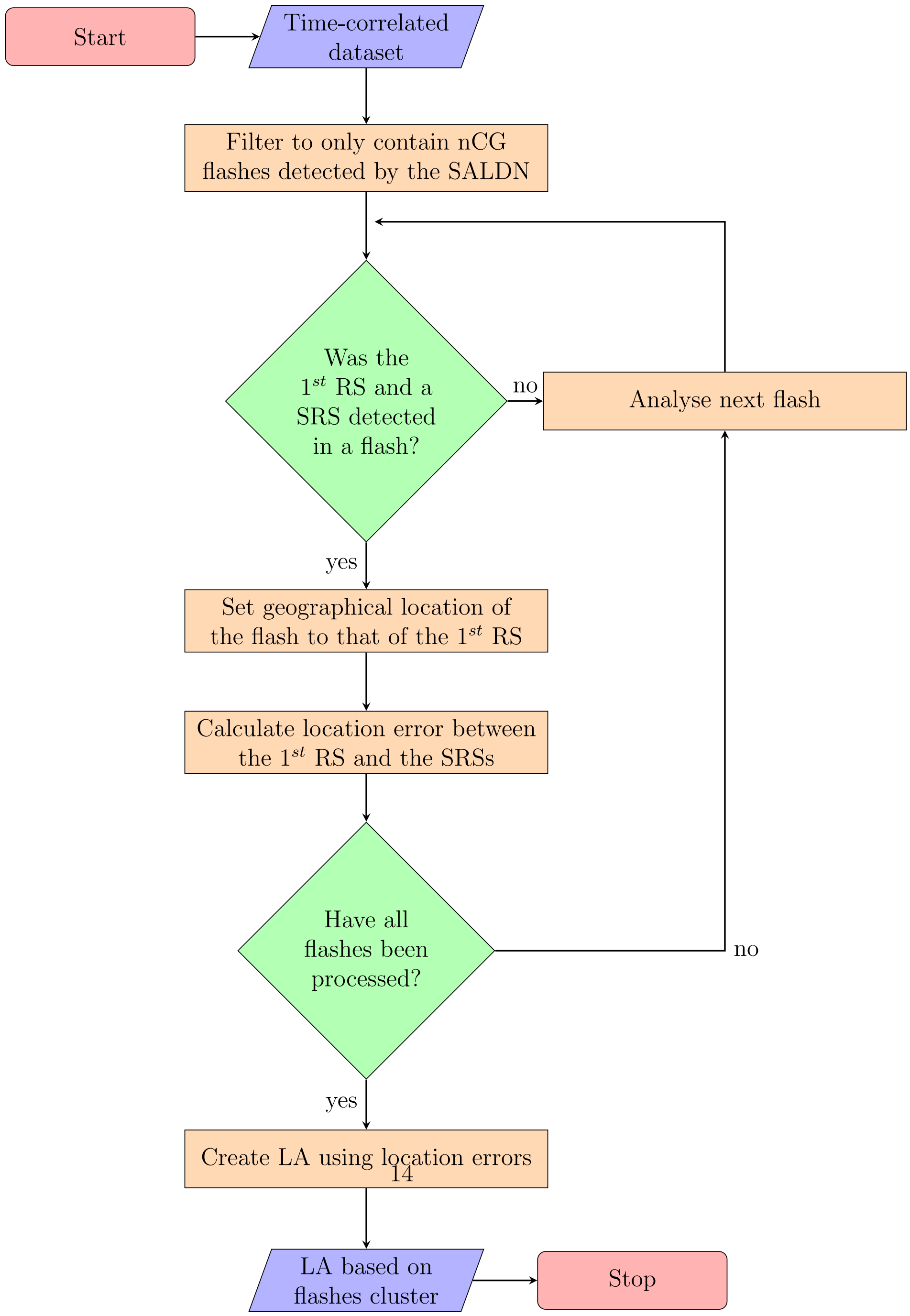

Fig. 7. Flow diagram of flash cluster algorithm.

Table 5
Location accuracy of the tower events.

Tower	N	Max	Min	Median	σ	Mode	Mean
Both towers	98	3847.3 m	4.9 m	**59.2 m**	423.0 m	4.9 m	152.2 m
Sentech Tower	45	1707.1 m	11.8 m	74.7 m	259.3 m	53.9 m	139.8 m
Telkom Tower	53	3847.3 m	4.9 m	51.0 m	522.9 m	4.9 m	162.8 m

6.2. Flash cluster

Fig. 13 shows the location accuracy distribution using the flash cluster method. The y-axis represents the number of SRSs and the x-axis represents the distance the SRSs are from the 1st return stroke. From the graph it can be seen that approximately 105 SRS are within 100 m of the 1st return stroke. This graph accounts for 241 SRSs out of a total of 245 SRSs. Therefore, four stroke reports had location errors greater than 2 km from the 1st return stroke. Table 8 shows the results of the flash cluster method. The table shows a median location accuracy of 124.4 m.

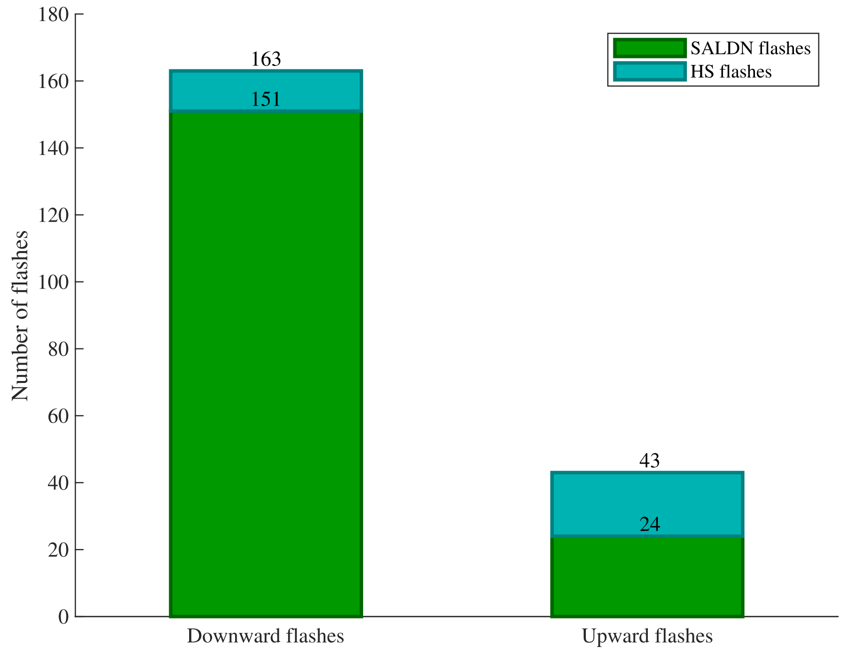

Fig. 8. Bar graph illustrating the number of downward and upward flashes captured on the high-speed cameras and detected by the SALDN.

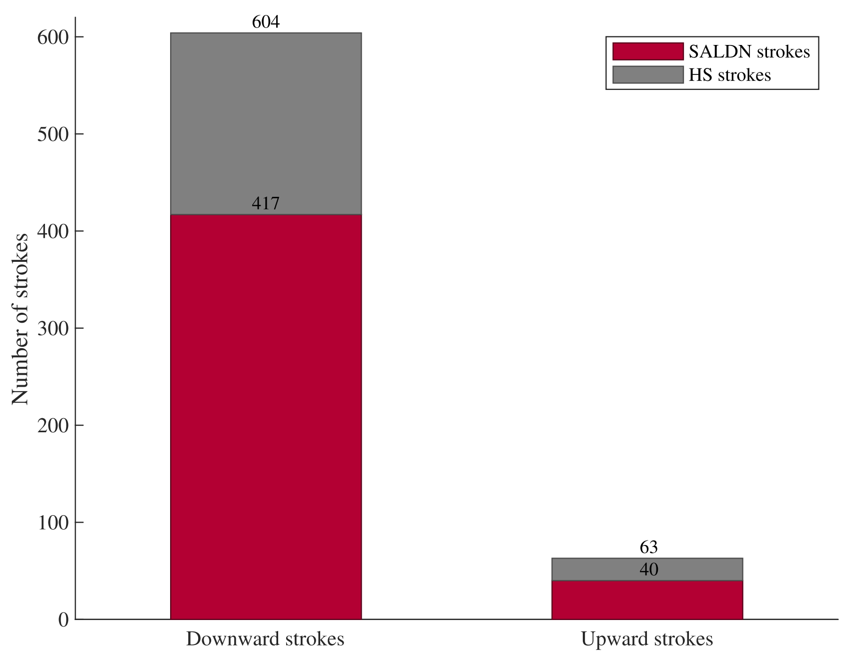

Fig. 9. Bar graph illustrating the number of downward and upward strokes captured on the high-speed cameras and detected by the SALDN.

Table 6
Location accuracy of Sentech Tower events.

Statistical parameters	Value
Count (N)	45
Median location error	74.7 m
Mean location error	139.8 m
10%	32.7 m
90%	212.6 m

Table 7
Location accuracy of Telkom Tower events.

Statistical parameters	Value
Count (N)	53
Median location error	51.0 m
Mean location error	162.8 m
10%	14.5 m
90%	307.9 m

7. Discussion

As shown in Table 4, the overall flash DE, including downward and upward flashes is 84.9%. Evaluating the DE of the flashes separately, the downward and upward flash DE were found to be 92.6% and 55.8% respectively. The greater DE of a downward flash is expected. 1st Return Strokes (RS) and Subsequent Return Strokes (SRS) have fast rise times, which aid in the detection of a flash. Upward flashes are not

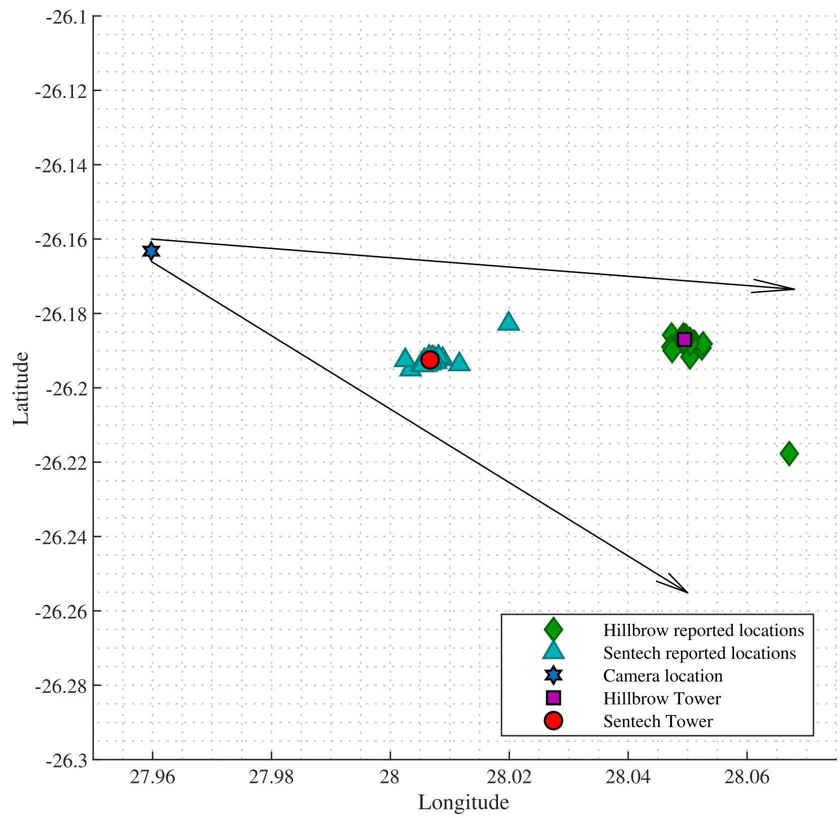

Fig. 10. Camera location and field of view with respect to the reported locations for the Telkom and Sentech Tower.

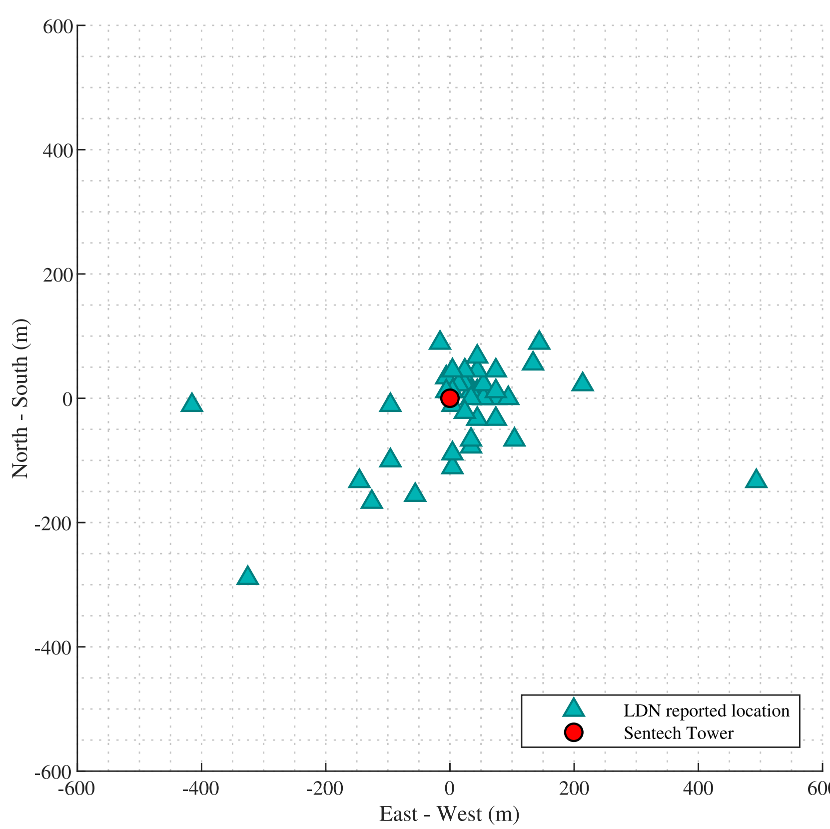

Fig. 11. Reported locations of lightning events, excluding one large location error, which occurred on the Sentech Tower.

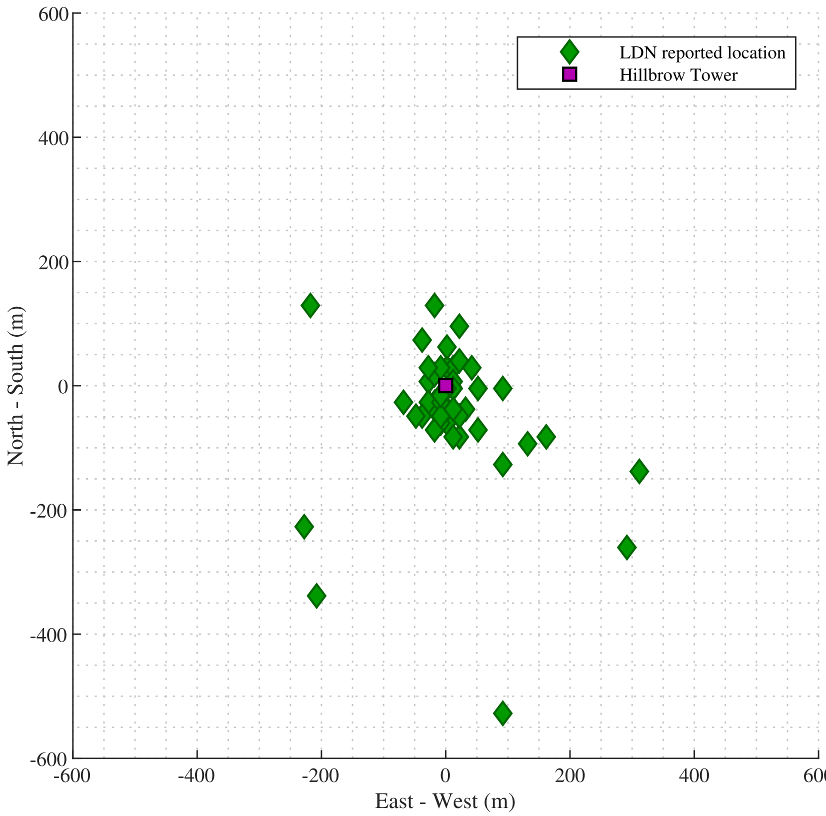

Fig. 12. Reported locations of lightning events, excluding one large location error, which occurred on the Telkom Tower.

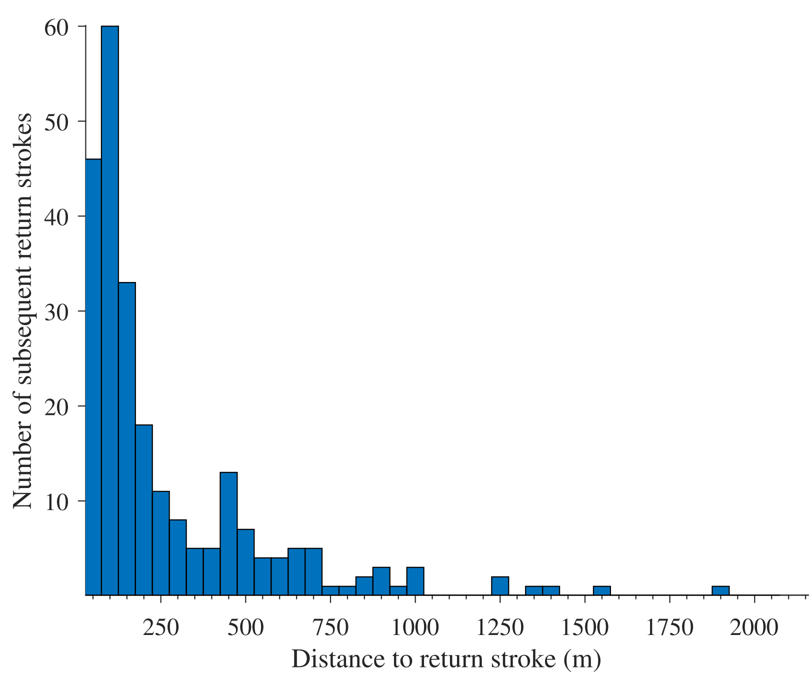

Fig. 13. Location accuracy distribution from flash cluster.

Table 8
Location accuracy from flash cluster method.

N	Max	Min	Median	σ	Mode	Mean
318	25711.3 m	0.0 m	**124.4 m**	1675.5 m	22.3 m	38.5 m

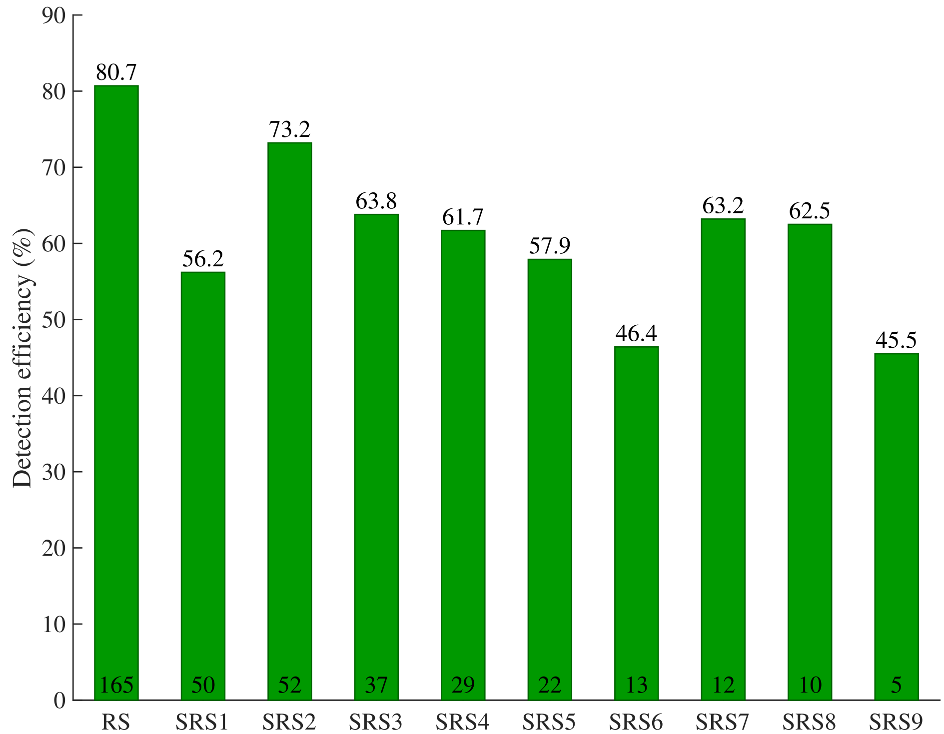

Fig. 14. Bar graph illustrating the detection efficiency of the strokes within negative cloud-to-ground flashes. The number within the bar represents the amount, of that specific stroke, detected by the SALDN.

expected to be detected by the SALDN due to the slow rise time of the upward leader, as can be seen in Table 4 where no upward leaders were detected by the SALDN. An upward flash is detected due to a strong Initial Continuous Current (ICC) pulse that is superimposed on the upward leader or the detection of a SRS after the upward leader. An evaluation of the SALDNs DE of downward flashes against that of upward flashes which contained SRSs can be performed. The SALDN detected 93.7% of upward flashes which contained SRSs as seen in Table 4. This value is very similar to that of downward flashes which are detected 92.6% of the time. However, the SALDN only detected 33.3% of upward flashes which did not contain SRSs. Therefore, SRSs increase the chances of an upward flash being detected by about 60%.

The overall stroke DE of the SALDN is 68.5% as seen in Table 4. This, as expected, is less than the flash DE since only one stroke needs to be detected to constitute the detection of a flash [7]. The SALDN DE of downward strokes and upward strokes is 69.0% and 63.4% respectively as seen in Table 4. These values are similar. This is expected since a SRS during an upward flash is similar to that of a SRS during a downward flash. This means that if an upward flash contains a SRS, it should have a very similar chance of being detected. This is in agreement with the results obtained where the flash DE of upward flashes containing SRSs is very similar to that of downward flashes. Fig. 14 shows the average detection efficiency of the strokes in negative cloud-to-ground flashes. The x-axis is the strokes in a flash and the y-axis is the detection efficiency. The 1st RS is seen to have the highest DE of 80.7% which is expected since this stroke should have the highest peak current within a flash. The DE decreases as the number of the SRS increases. The number of strokes detected for each stroke category on the x-axis is shown at the bottom of each bar. For instance there was 165 detected 1st RSs. The 1st RSs had a detection efficiency of 80.7%.

The median LA of the SALDN using the location of known attachment and flash cluster method is 59.2 m and 124.4 m respectively. As seen in Fig. 10, the locations of known attachment were the Telkom and Sentech Tower. It must be noted that the majority of flashes which terminated on these towers were upward flashes. Therefore, the data for this method consists of detected ICC pulses and mostly SRS. There was a small amount of 1st return strokes which occurred on the towers. It was seen that there were outliers for both towers. These outliers were time-correlated with the events that were filmed attaching to the towers. However, the SALDN reported location had large location errors. The subsections below will discuss these outliers and explain why they occurred.

7.0.1. Sentech Tower outlier

The Sentech Tower outlier seen in Fig. 10 can be examined using Fig. 15. At the time in which the SALDN detected a lightning event, there was an IC flash which appeared as seen in Fig. 15. Within the same millisecond of this IC flash there was an ICC pulse. Therefore according to the way the data were time-correlated, this ICC pulse was considered as detected. However, it was the nearby IC that was detected. At no point did the IC connect with the upward leader channel causing an ICC pulse. This IC was situated over the Telkom Tower. This is in agreement with the location of the outlier in Fig. 10 where the outlier is almost in line with the Telkom Tower looking from the perspective of the camera. The SALDN estimated the peak current of the IC flash to be −5 kA. This is relatively small and coincides with being an IC event [14]. Therefore, in this instance, it seems that the SALDN misclassified an IC event as a CG stroke.

7.0.2. Telkom Tower outlier

The outlier which is seen in Fig. 10 can be explained by using the images seen in Fig. 16. The upward flash in question was of a negative polarity, in other words a positive upward leader. In the first image of Fig. 16 an attempted ICC pulse can be seen occurring on the Telkom Tower. In the second image, a positive SRS makes attachment with the negative attempted ICC pulse in mid-air. The SALDN detected this attachment giving the geographical location of the outlier seen in Fig. 10 with a peak current of +41 kA. Fig. 10 shows that the reported location of the outlier is to the right of the tower from the cameras perspective. This agrees with where the attachment took place in the second image in Fig. 16.

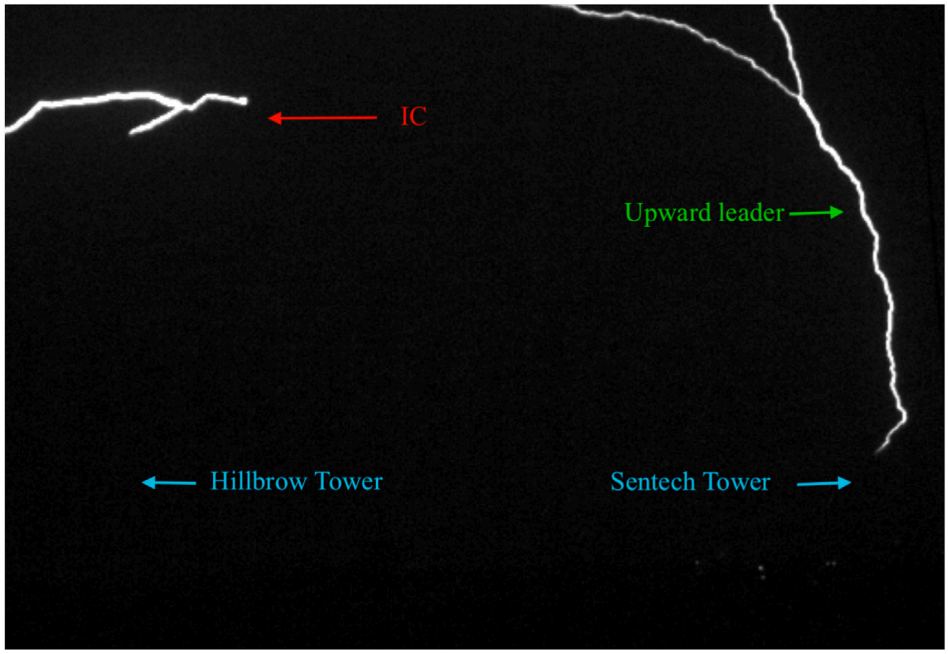

Fig. 15. Image explaining the outlier in the Sentech Tower data.

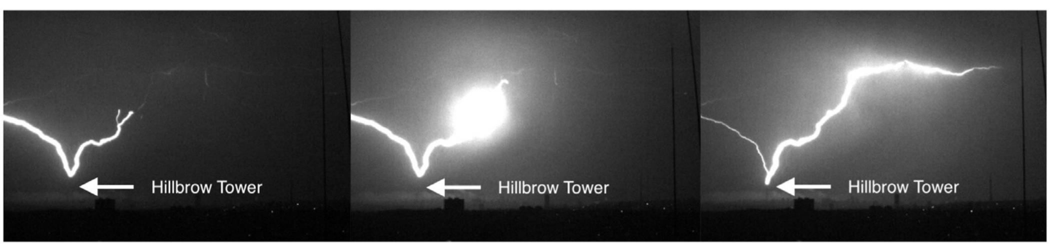

Fig. 16. Sequence of images explaining the Telkom Tower outlier.

Additionally, the chi-square value for this SALDN entry was reported to be 1.7. This is relatively high. Fig. 3 gives an indication of the chi-square values of strokes. The chi-square value is one of the parameters used to describe the quality of the geographical location reported by a LLS [15]. This high chi-square value indicates a greater level of uncertainty to the geographical location reported for this outlier. These figures and chi-square values explain the outlier event which occurred 3.8 km from the tower.

7.1. Flash cluster

The flash cluster method collects the location errors between the 1st RS and the SRSs of the same flash. The location errors are calculated from the SALDN reported locations. It was discussed in the methodology Section 4.3.2 that the 1st RS in a flash generally has the highest peak current compared to the SRSs. This makes it in most cases, the most accurately located stroke in a flash. Fig. 17 shows the mean peak current as a function of stroke order up to a multiplicity of 10. The x-axis is the strokes in the flashes and the y-axis is the average reported peak current. The number of strokes detected for each stroke category on the x-axis is shown at the bottom of each bar. It can be seen that the 1st RS has, on average, the highest peak current values. This confirms the use of the 1st RS as the location of the flash in this method.

This figure also follows a similar trend to the one seen in Fig. 14 where the DE of the strokes in a flash are illustrated. Fig. 17 agrees with Fig. 14 since the 1st return stroke has the highest reported peak current and is also the stroke detected most often. The shape of the graphs are also similar confirming the relationship between the peak current of a stroke and the detection efficiency.

7.2. Comparison of location accuracy methods

The two location accuracy methods can be compared. Table 9 below compares the results of the locations of known attachment method versus the flash cluster method. It can be seen that the flash cluster method has a median location accuracy which is 65.2 m greater than that of the known location terminations. However, as described in Ref. [12] the flash cluster method provides the upper bounds of the location accuracy due to the fact that the ground strike points within a flash cluster may vary slightly.

Based on these results the flash cluster method is a suitable method for finding the LA of a LLS. This method can be used if there are no locations of known attachment. It is also easier to gather data for the flash cluster method because all that is needed is high-speed videos of flashes as opposed to high-speed videos of flash terminating on specific locations.

7.3. SALDN performance evaluation comparison

This section compares the performance evaluation of the SALDN to the performance evaluations of the studies presented previously. Table 10, shows the results for the studies compared to the SALDN. The SALDN (Overall) row refers to the overall DE (upward and downward flashes) of the SALDN. The overall LA value in this row is from the location of known attachments method. The SALDN (Downward flashes only) row refers to the DE of the SALDN for downward flashes. The LA value in this row is from the flash cluster method.

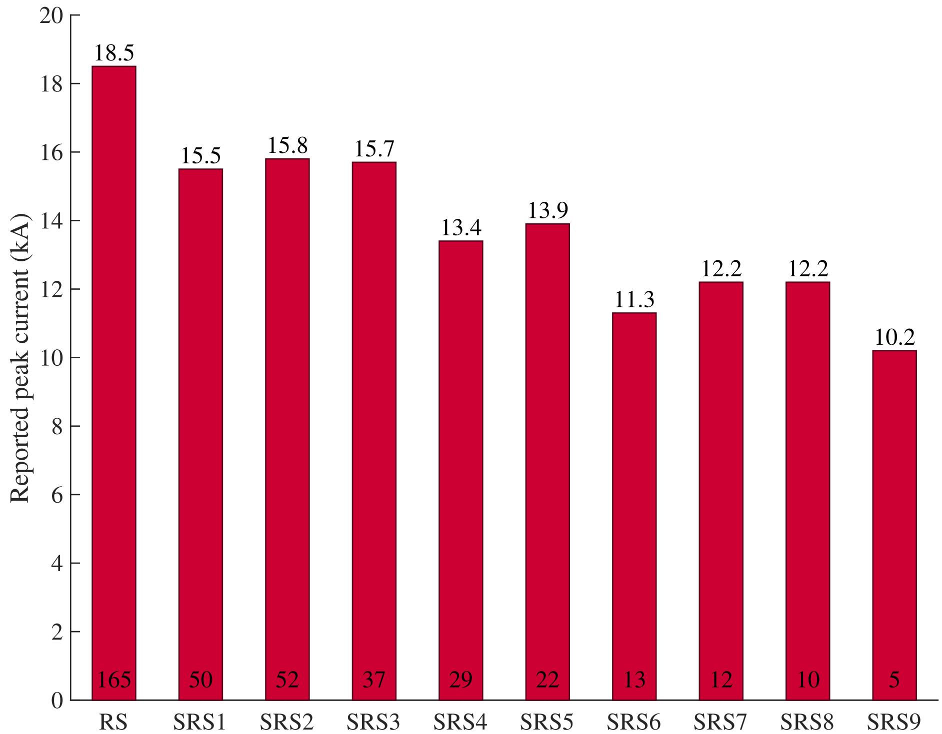

Fig. 17. Bar graph illustrating the average peak current reported for the strokes within negative cloud-to-ground flashes. The number within the bar represents the amount, of that specific stroke, detected by the SALDN.

Table 9
Comparison of location accuracy methods.

Method	N	Max	Min	Median	σ	Mode	Mean
Both towers	98	3847.3 m	4.9 m	**59.2 m**	423.0 m	4.9 m	152.2 m
Flush cluster	318	25711.3 m	0.0 m	**124.4 m**	1675.5 m	22.3 m	38.5 m

Table 10
Comparison of SALDN performance evaluation to other studies.

LLS	Flash DE	Stroke DE	Median LA
EUCLID [8]	98%	84%	89 m
GHMLLS [6]	95%	90%	410 m
RINDAT [9]	87%	55%	3400 m
NLDN [10]	94%	75%	309 m
SALDN (Overall)	85%	69%	59 m
SALDN (Downward flashes only)	93%	69%	124 m

The DE of downward flashes for the SALDN is more in-line with the flash DE of the studies. The LA values obtained from the locations of known attachment and the flash cluster method show how well the SALDN locates lightning events. The results show that the ground-flash density map accuracy in South Africa is similar to those seen in other countries. This result also gives information on how accurate the ground strike point density maps would be with the SALDN data. The results of the SALDN performance evaluation can be compared to the performance evaluation completed in 2014 [1]. In 2014, the overall flash DE was found to be 76% in the last season, this value has now increased to an overall flash DE of 85%. However, the study in 2014 would have been an underestimate of the overall flash DE of the SALDN. The majority of flashes analysed were upward flashes because the ground truth data were collected from lightning events terminating on the Sentech Tower. As discussed previously, it is not expected that an LLS will detect upward flashes without any SRS because of the slow rise time of the upward leader. The median location accuracy in 2014 was found to be 280 m based on data over the past 4 years. This has now reduced to 59 m. This shows the improvement of the SALDN over the last 5 years.

7.4. *Interesting cases*

A number of interesting cases were observed. There were upward triggering events seen on the camera and detected by the SALDN which showed nearby-lightning-triggered upward flashes, a certain percentage of M-components and ICC pulses were detected as strokes by the SALDN and there were a number dual strokes SALDN entries.

7.4.1. *Upward triggering event*

There are two types of upward flashes: nearby-lightning-triggered upward flash and self-initiated upward flash [16]. This section will discuss the amount of CG nearby-lightning-triggered flashes that was seen on camera and/or detected by the SALDN. Of the 43 upward flashes seen in the high-speed camera footage, 14 had a nearby CG triggering event. Of the 14 triggering events, 6 were seen on the high-speed camera and were detected by the SALDN. The remaining 8 triggering events were out of the field of view of the camera but were detected by the SALDN as a positive CG flashes. Although these detected triggering events were out of view, the upward leader being

Table 11
Upward flash triggering events detected by the SALDN and out of view from the cameras.

Count	Tower of flash	Distance to Sentech Tower	Distance to Telkom Tower	Timing of trigger	Estimated current
1	Sentech	**14.1 km**	–	60 ms before	21 kA
2	Both	**5.8 km**	**6.2 km**	1 ms during	50 kA
3	Telkom	–	**14.5 km**	253 ms during	31 kA
4	Sentech	**14.6 km**	–	12 ms before	64 kA
5	Sentech	**33.7 km**	–	629 ms before	11 kA
6	Both	**14.0 km**	**18.2 km**	7 ms before	106 kA
7	Sentech	**22.0 km**	–	60 ms before	54 kA
8	Telkom	–	**21.2 km**	42 ms before	28 kA

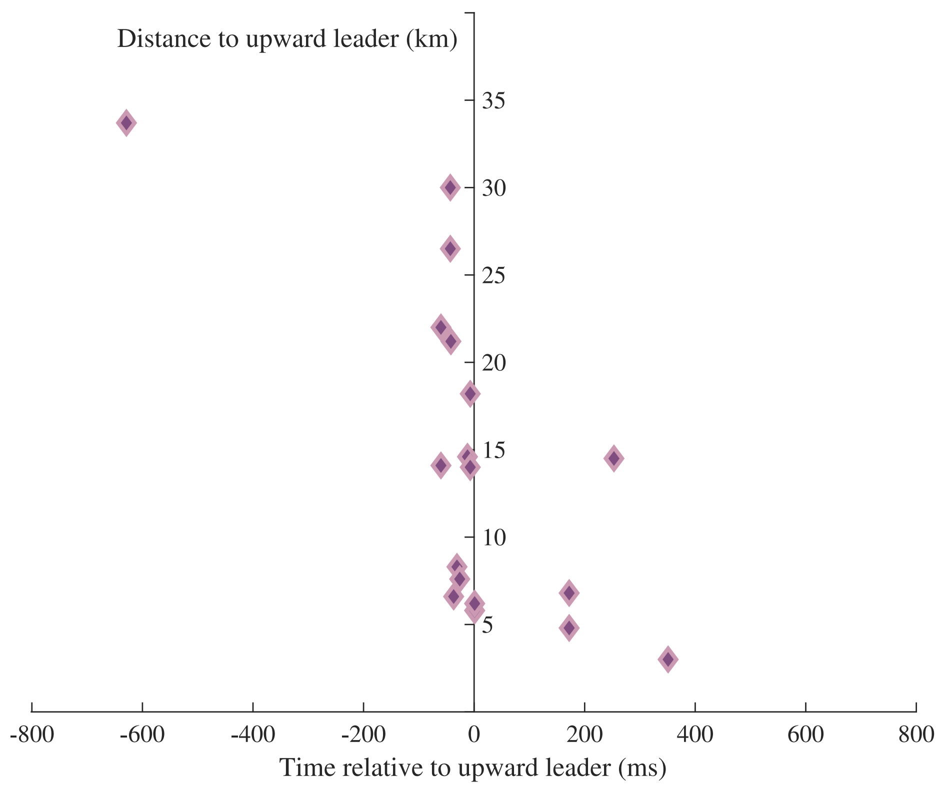

Fig. 18. Scatter plot illustrating the triggering events with respect to the distance from the tower and the time to initiate the upward leader.

Table 12
The amount of ICC pulses and M-components captured with the high-speed camera and detected by the SALDN.

Lightning events	High-speed camera	SALDN
M-components	111	15
ICC pulses	387	57
Total	498	72

initiated from the Telkom and Sentech Tower was still seen on the high-speed camera. Table 11 below shows the triggering events detected by the SALDN that were out of view of the high-speed camera. "Tower of flash" refers to the tower from which the upward leader was initiated. The distance between the trigger event and the Sentech and Telkom Tower is included in the table and the "Timing of trigger" refers to when the trigger occurred in relation to when the upward leader was seen on the high-speed camera. "Estimated current" is the current value of the triggering event, measured by the SALDN.

Fig. 18 below is a scatter plot containing all 14 nearby-lightning-triggered upward flashes. Of the 14 upward flashes, 4 of them had upward leaders on both of the towers. The figure illustrates the distance the trigger event was to the towers versus the timing of the trigger events (when the upward leader was initiated). If the triggering events in Fig. 18 are to the left of the y-axis, the triggering events occurred before the upward leader was initiated. If the triggering events are to the right of the y-axis, the triggering event occurred during the upward flash — this is because of leader activity inside the cloud as described in [17]. The y-axis illustrates how far the triggering event was from a tower. In Fig. 18, 14 of the 18 triggering events are to the left of the y-axis while the remaining 4 are to the right of the y-axis. Therefore, according to the data in the figure, 77.8% of nearby-lightning-triggered upward flashes are initiated from downward flashes which occur before the initiation of the upward leader. It is important to note that the remaining 29 upward flashes are not necessarily self-initiated. Of the 29 upward flashes, some might have been triggered by IC lightning. Additionally, the SALDN might not have detected some of the triggering events outside of the field of view and the triggering events might have been on the outside of the coordinates to which the SALDN was filtered by. Therefore, this data is only to show an estimate of the number of CG nearby-lightning-triggered upward flashes in this dataset. The detection of a CG triggering event in an upward flash is not strictly a detection of an upward flash. Therefore, in this research, a detected CG triggering event was classified as a downward flash.

Table 13
Dual stroke entries from the SALDN.

Dual stroke entry	Polarity	Time	Latitude	Longitude	Peak current (kA)
1	Positive	18:46:27.321	−26.2313	28.0727	50
		18:46:27.321	−26.2297	28.0729	52
2	Negative	20:05:13.575	−26.2073	28.0800	−16
		20:05:13.575	−26.2073	28.0800	−16
3	Negative	20:24:47.100	−26.2520	28.2096	−13
		20:24:47.100	−26.2520	28.2096	−13
4	Negative	20:28:35.709	−26.2349	28.1947	−16
		20:28:35.709	−26.2339	28.1945	−17
5	Negative	15:46:51.678	−26.1863	28.0491	−27
		15:46:51.678	−26.1867	28.0494	−24
6	Positive	18:44:39.426	−26.1554	27.9289	28
		18:44:39.426	−26.1535	27.9291	27
7	Negative	14:45:50.361	−26.2016	28.0368	−36
		14:45:50.361	−26.2026	28.0352	−34
8	Negative	14:51:13.770	−26.2025	28.0312	−12
		14:51:13.770	−26.2047	28.0288	−14
9	Positive	18:52:19.801	−26.1488	28.1130	37
		18:52:19.801	−26.1586	28.1124	40
10	Positive	18:32:48.994	−26.2680	28.1506	38
		18:32:48.994	−26.2664	28.1507	34

7.4.2. Detected M-components and ICC pulses

In the *time-correlated dataset* it was observed that the SALDN stroke data detected M-components and ICC pulses. M-components and ICC pulses are not considered strokes since they are transient effects which occur during the CC or ICC phase. The total number of M-components (for downward and upward flashes) and ICC pulses the SALDN detected is 15 and 57 respectively as seen in Table 4. The total number of M-components (for downward and upwards flashes) and ICC pulses in the high-speed camera data is 111 and 387 respectively. Therefore 13.5% of M-components and 14.7% of ICC pulses are classified as strokes. These values are very similar which is expect since M-components are similar to ICC pulses as discussed by Flache et al. (2008) [18]. The numbers have been summarised in Table 12 below. The total number of M-components and ICC pulses that were filmed by the high-speed camera is 498. The total number of M-components and ICC pulses that were detected by the SALDN is 72. The SALDN classified 14.5% of M-components and ICC pulses as CG strokes.

7.5. SALDN dual stroke entry

Throughout the study, dual stroke entries in the CG stroke SALDN data were observed. The dual stroke entries were two strokes detected at the same millisecond, with a similar geographical location and similar peak current values. The dual stroke entries are shown in Table 13 below. Entry 5 is a SRS in an upward flash. The remaining entries were strokes in a downward flash. Of the 10 entries, 6 were of negative polarity and 4 were of positive polarity. These dual strokes entries did not present any difference with regards to the high-speed camera footage of other strokes which were analysed. If a dual stroke entry occurred in the data, the stroke with the highest peak current was chosen.

8. Conclusion

Lightning location systems provide information about lightning events in many countries. The South African Lightning Detection Network has not had a performance evaluation where the flash detection efficiency, stroke detection efficiency and location accuracy are compared with ground-truth high-speed video footage of lightning. Results show that the South African Lightning Detection Network has a flash detection efficiency of 84.9%, stroke detection of 68.5% and has a median location accuracy of 59.2 m. The location accuracy was found using ground truth lightning events which occurred on structures with known locations. Additionally, the location accuracy was found using locations errors within a flash cluster which produced a median location accuracy of 124.4 m, however this is regarded as the upper bound of the location accuracy of the South African Lightning Detection Network. Interesting cases regarding upward triggering events, detected M-components and initial continuing current pulses and dual South African Lightning Detection Network stroke entries were discussed.

CRediT authorship contribution statement

Haydn Fensham: Data curation, Formal analysis, Methodology, Visualization, Writing – review & editing. **Hugh G.P. Hunt:** Conceptualization, Funding acquisition, Investigation, Resources, Software, Validation, Writing – review & editing. **Carina Schumann:** Conceptualization, Data curation, Formal analysis. **Tom A. Warner:** Resources, Writing – review & editing. **Morne Gijben:** Resources, Writing – review & editing.

Declaration of competing interest

The authors declare that they have no known competing financial interests or personal relationships that could have appeared to influence the work reported in this paper.

Data availability

The authors do not have permission to share data.

Acknowledgements

This work is based on the research supported in part by the National Research Foundation of South Africa and their support of the Johannesburg Lightning Research Laboratory through the Thuthuka programme (Unique Grant No.: 122038) and by DEHNAFRICA and their support of the Johannesburg Lightning Research Laboratory. The authors would like to thank the South African Weather Service (SAWS) for their support and for providing the SALDN data used in this paper, specifically Morné Gijben and Rydall Jardine.

References

[1] H.G.P. Hunt, Y.C. Liu, K.J. Nixon, Evaluation of the South African lightning detection network using photographed tall tower lightning events from 2009–2013, in: International Conference on Lightning Protection, ICLP, 2014.

[2] C. Schumann, H.G. Hunt, J. Tasman, H. Fensham, K.J. Nixon, T.A. Warner, M.M. Saba, High-speed video observation of lightning flashes over Johannesburg, South Africa 2017–2018, in: 2018 34th International Conference on Lightning Protection, ICLP, 2018, pp. 1–7.

[3] H. Fensham, C. Schumann, H. Hunt, J. Tasman, K. Nixon, T. Warner, M. Gijben, Performance evaluation of the SALDN using highspeed camera footage of ground truth lightning events over Johannesburg, South Africa, in: 2018 34th International Conference on Lightning Protection, ICLP, 2018, pp. 1–5.

[4] H.G. Hunt, C. Schumann, J.R. Smit, C. Gomes, K.J. Nixon, I.R. Jandrell, M.M. Saba, T.A. Warner, The johannesburg lightning research laboratory, in: 2021 35th International Conference on Lightning Protection (ICLP) and XVI International Symposium on Lightning Protection, Vol. 1, SIPDA, 2021, pp. 01–07.

[5] D.R. Poelman, W. Schulz, S. Pedeboy, D. Hill, M. Saba, H. Hunt, L. Schwalt, C. Vergeiner, C.T. Mata, C. Schumann, T. Warner, Global ground strike point characteristics in negative downward lightning flashes – Part 1: Observations, Nat. Hazards Earth Syst. Sci. 21 (6) (2021) 1909–1919, URL https://nhess.copernicus.org/articles/21/1909/2021/.

[6] Y. Zhang, W. Lu, Y. Zhang, D. Zheng, L. Chen, S. Chen, X. Yan, Evaluation for the performance of the Guangdong-Hongkong-Macau Lightning Location System, in: 23rd International Lightning Detection Conference, 2014.

[7] H.G.P. Hunt, K.J. Nixon, I.R. Jandrell, Comparison between south african lightning detection network interpretation of single- channel and branched upward lightning flashes to a tall structure, in: 2013 International Symposium on Lightning Protection (XII SIPDA), Belo Horizonte, Brazil, October, 2013.

[8] W. Schulz, G. Diendorfer, S. Pedeboy, D.R. Poelman, The European lightning location system EUCLID – Part 1: Performance analysis and validation paper, Nat. Hazards Earth Syst. Sci. (2016).

[9] M.G. Ballarotti, M.M.F. Saba, O. Pinto, A new performance evaluation of the Brazillian Lightning Location System (RINDAT) based on high-speed camera observations of natural negative ground flashes, 2006.

[10] S. Mallick, V.A. Rakov, T. Ngin, W.R. Gamerota, J.T. Pilkey, J.D. Hill, M.A. Uman, D.M. Jordan, J.A. Cramer, A. Nag, An update on the performance characteristics of the NLDN, in: 23rd International Lightning Detection Conference, 2014.

[11] M. Gijben, The lightning climatology of South Africa, S. Afr. J. Sci. 108 (3/4) (2012) 10, Art. 740.

[12] W. Schulz, C. Vergeiner, H. Pichler, G. Diendorfer, K.L. Cummins, Location accuracy evaluation of the Austrian Lightning Location System ALDIS, in: 22nd International Lightning Detection Conference, ILDC, 2012.

[13] W. Schulz, Performance Evaluation of Lightning Location Systems (Dissertation), Universitat Wien Fakultat fur Elektrotechnik, 1997.

[14] K.L. Cummins, M.J. Murphy, An overview of lightning locating systems: history, techniques, and data uses, with an in-depth look at the U.S. NLDN, IEEE Trans. Electromagn. Compat. 51 (3) (2009).

[15] A. Nag, M.J. Murphy, W. Schulz, K.L. Cummins, Lightning locating systems: Insights on characteristics and validation techniques, Earth Space Sci. 2 (4) (2015) 65–93.

[16] H. Zhou, G. Diendorfer, R. Thottappillil, H. Pichler, M. Mair, Measured current and close electric field changes associated with the initiation of upward lightning from a tall tower, J. Geophys. Res.: Atmos. 117 (D8) (2012).

[17] C. Schumann, M.M.F. Saba, T.A. Warner, M.A.S. Ferro, J.H. Helsdon, R. Thomas, R.E. Orville, On the triggering mechanisms of upward lightning, Sci. Rep. 9 (1) (2019) 9576, URL https://doi.org/10.1038/s41598-019-46122-x,

[18] D. Flache, V.A. Rakov, F. Heidler, W. Zischank, R. Thottappillil, Initial-stage pulses in upward lightning: Leader/return stroke versus M-component mode of charge transfer to ground, Geophys. Res. Lett. 35 (13) (2008).